ACS APPLIED MATERIALS & INTERFACES

Research Article

www.acsami.org

Effects of Substrate on Piezoelectricity of Electrospun Poly(vinylidene fluoride)-Nanofiber-Based Energy Generators

Byoung-Sun Lee,[†,+] Boongik Park,[‡,+] Ho-Sung Yang,[§] Jin Woo Han,[∥] Chweelin Choong,[†] Jihyun Bae,[†] Kihwan Lee,[‡] Woong-Ryeol Yu,[§] Unyong Jeong,[⊥] U-In Chung,[†] Jong-Jin Park,*[,†] and Ohyun Kim*[,‡]

[†]Samsung Advanced Institute of Technology, Yong-in 449-712, Republic of Korea

[‡]Department of Electrical Engineering, Pohang University of Science and Technology (POSTECH), Pohang 790-784, Republic of Korea

[§]Department of Materials Science and Engineering, Seoul National University, Seoul 151-744, Republic of Korea

[∥]Samsung Corning Precision Materials, Gumi 730-360, Republic of Korea

[⊥]Department of Materials Science and Engineering, Yonsei University, 134 Chinchon-Dong, Seoul 120-749, Republic of Korea

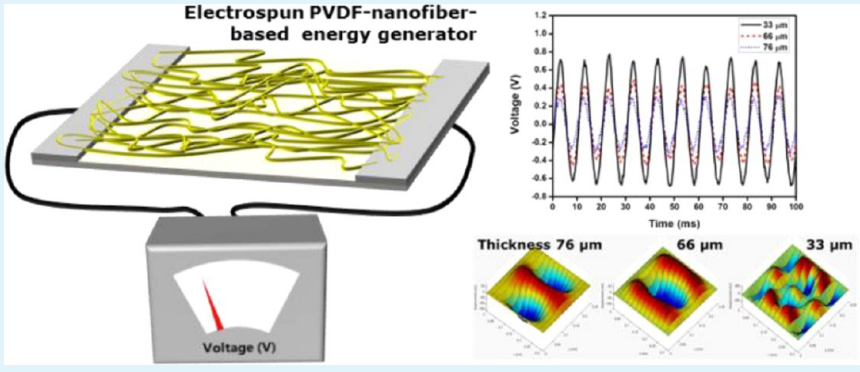

ABSTRACT: We report the effects of various substrates and substrate thicknesses on electrospun poly(vinylidene fluoride) (PVDF)-nanofiber-based energy harvesters. The electrospun PVDF nanofibers showed an average diameter of 84.6 ± 23.5 nm. A high relative β-phase fraction (85.2%) was achieved by applying high voltage during electrospinning. The prepared PVDF nanofibers thus generated considerable piezoelectric potential in accordance with the sound-driven mechanical vibrations of the substrates. Slide glass, poly(ethylene terephthalate), poly(ethylene naphthalate), and paper substrates were used to investigate the effects of the intrinsic and extrinsic substrate properties on the piezoelectricity of the energy harvesters. The thinnest paper substrate (66 μm) with a moderate Young's modulus showed the highest voltage output (0.4885 V). We used high-performance 76, 66, and 33 μm thick papers to determine the effect of paper thickness on the output voltage. The thinnest paper substrate resulted in the highest voltage output (0.7781 V), and the numerical analyses of the sound-driven mechanical deformation strongly support the hypothesis that substrate thickness has a considerable effect on piezoelectric performance.

KEYWORDS: *poly(vinylidene fluoride), electrospun nanofiber, piezoelectric nanogenerator, paper*

1. INTRODUCTION

Rechargeable power and renewable energy sources have recently attracted significant attention because of deepening concerns about the fossil fuel depletion and pollution caused by excessive energy consumption. Various forms of reusable energy—such as electrical power sources (i.e., energy harvesters)—are promising solutions to these problems. Using nanomaterials to convert various energies (such as solar, wind, thermal, tidal, etc.) into electrical energy has been researched extensively.[1−4] Mechanical vibration is a renewable energy more abundant than many other sources since all movements from atoms to the earth produce mechanical vibration. Sound waves are mechanical vibrations propagating through air and are both the most abundant and most wasted energy. For example, train, airplane, and car sounds produce mechanical vibrations in the order of tens to hundreds of decibels.[5]

Piezoelectric materials are materials that accumulate electrical charge in response to applied mechanical stress. They can be classified as natural (e.g., berlinite,[6] quartz,[7] topaz,[8] etc.) or synthetic (e.g., $BaTiO_3$,[9] $PbTiO_3$,[10] lead zirconate titanate (PZT),[11] ZnO,[12] poly(vinylidene fluoride) (PVDF),[13] etc.). $BaTiO_3$, PZT, ZnO, and PVDF are the most widely investigated piezoelectric materials owing to their superior piezoelectric performance.[14] PVDF was recently used as the core material in a wearable/implantable piezoelectric transducer

Received: December 10, 2013
Accepted: February 13, 2014
Published: February 13, 2014

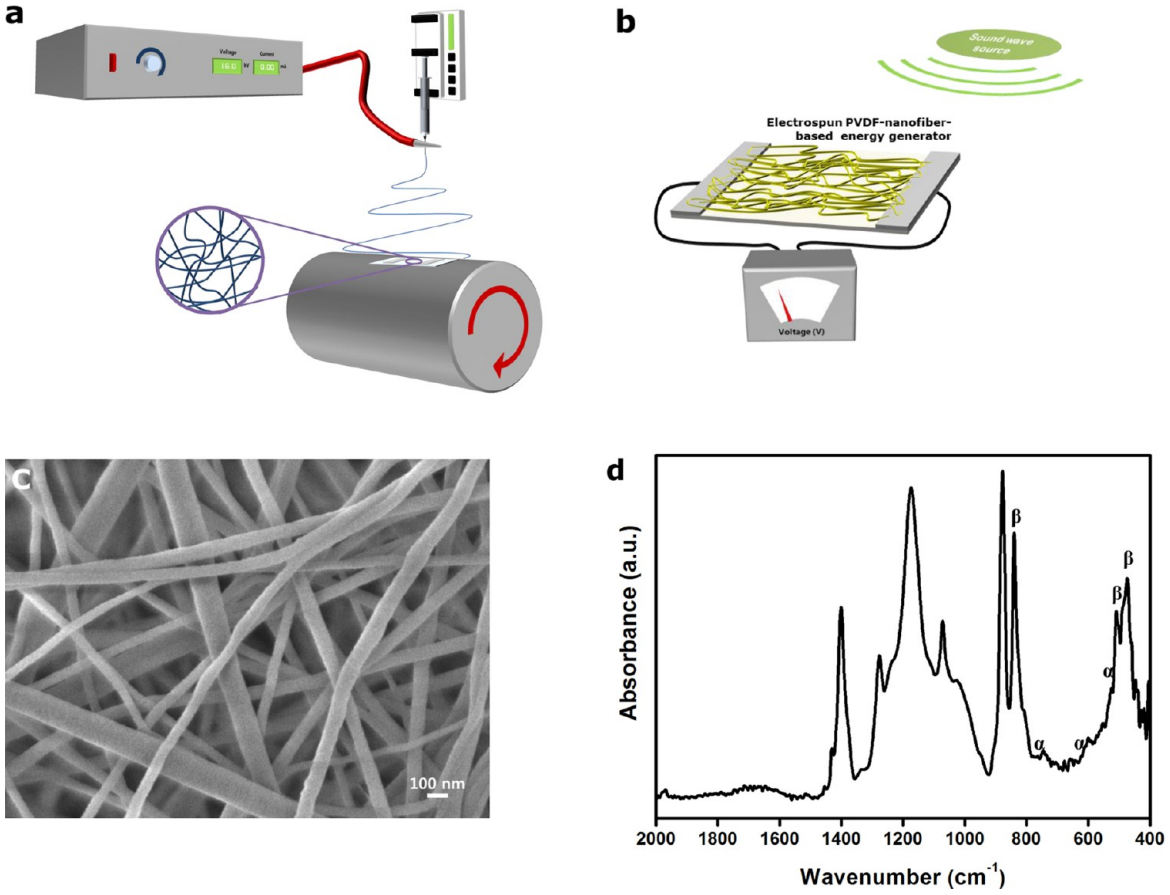

Figure 1. Schematics of the (a) electrospinning setup and (b) nanogenerator. (c) SEM image of electrospun PVDF nanofiber morphology. (d) FT-IR spectrum showing peaks associated with the α and β phases.

because it is malleable,[13,15] and it is lightweight,[16] flexible,[17] stretchable,[17] and biocompatible.[18] The mechanical-stress-induced microstructural deformation of piezoelectric transducers produces dipole moments that generate differences in potential at both transducer ends. Kawai first demonstrated the tensile piezoelectricity in stretched and poled PVDF films in 1969.[19] Uniaxially oriented PVDF exhibits relatively weak electromechanical coupling and shows a piezoelectric coefficient of -33 pC·N^{-1}, significantly poorer than inorganic perovskite piezoelectrics.[20,21] This limitation apparently stems from randomly oriented H−C−F dipoles, as untreated PVDF can contain α and β crystalline phases. The nonpolar α phase, consisting of randomly oriented dipoles, forms most readily when PVDF is cooled above the glass-transition temperature (T_g), while the well-oriented dipoles form the piezoelectric β phase.[22] Thus, post-treating PVDF to convert the α into the β phase improves piezoelectric performance. However, it is also costly and time-consuming, so this step is usually omitted when piezoelectric nanogenerators are fabricated in an industrial setting. Researchers have recently observed in situ the relationship between the mechanical stretching and electrical poling of piezoelectric nanogenerators and used direct-written (or near-field electrospun) PVDF nanofibers to transform the α phase into the polar β phase at a high voltage.[23−25] Moreover, Nasir et al. systematically investigated the microstructural phases of electrospun PVDF nanofibers,[26] which may be the optimal material for improving the performance of piezoelectric nanogenerators. Nanogenerator substrates can greatly affect the performance of nanomaterial-based piezoelectric transducers. Thin-film structured substrates can effectively convert sound waves into mechanical vibration and eventually transfer the mechanical vibration to the electrospun PVDF nanofibers. Therefore, combining sound waves and piezoelectric transducers may facilitate the use of mechanical vibration as electrical energy because sound wave sources are abundant and piezoelectric materials exhibit effective energy-conversion mechanisms. To our knowledge, the effects of various substrates and their thicknesses on PVDF-nanofiber-based piezoelectric nanogenerators have not been investigated to date. Therefore, we systematically analyzed the effects of the Young's moduli and thicknesses of various substrates on PVDF nanofiber piezoelectricity and identified the optimal substrate for application in energy harvesters.

2. EXPERIMENTAL SECTION

Electrospinning PVDF Nanofibers. The PVDF solution was produced from PVDF powder (M_w = 534 000 g/mol) (Sigma-Aldrich), *N*,*N*-dimethylformamide (DMF) (Sigma-Aldrich), acetone (Sigma-Aldrich), and ZonylUR (DuPont), which is an anionic phosphate fluorosurfactant that was provided without solvents. All reagents were used as purchased. The solution consisted of 16, 80, and 4 wt % PVDF, solvent (DMF:acetone = 4:6), and fluorosurfactant, respectively. The acetone and fluorosurfactant were used to improve the evaporation and reduce the surface tension of the solution,[27] which was homogenized at 100 °C for 1 day by stirring. Slide glasses (1125 μm thick), poly(ethylene terephthalate) (PET) film (255 μm thick), poly(ethylene naphthalate) (PEN) (105 μm thick), and 33, 66, and 76 μm thick papers whose densities were 25, 52, and 80 g/m^2 (OJI Specialty, View Corona), respectively, were used as the substrates. The

dx.doi.org/10.1021/am405684m | ACS Appl. Mater. Interfaces 2014, 6, 3520−3527

PVDF solution was electrospun at 0.5 mL/h onto the various substrates rotating at 800 rpm. The tip-to-collector distance was 15 cm, and the applied voltage was 15 kV. The electrospun nanofibers were collected onto two grounded aluminum electrodes on the substrates, which were separated by a 2.5 cm gap.

Characterization. The morphologies of the electrospun nanofibers were observed using scanning electron microscopy (SEM, S-4700). The sound waves were generated using a speaker and a function generator (Tektronix, CFG280), and the intensity of the generated sound was measured using a decibel meter. The effects of the sound waves on nanogenerator performance were assessed using an oscilloscope (Agilent, MS07054A). Fourier-transform infrared spectrometry (FT-IR, Jasco) was used in the 400−2000 cm^{-1} range to generate IR spectra for the electrospun fibers.

Simulation. The effects of substrate thickness on nanogenerator performance were simulated numerically. A nanogenerator on a paper substrate and a single straight PVDF filament laid across the two Al electrodes were assumed for simplicity.[28] The boundary-element method was used to solve nonsingular boundary integral equations to analyze piezoelectric performance on the basis of the free vibration of the paper substrate.[29] A simply supported, 25 mm long, 31 mm wide rectangular plate was assumed to evaluate the vibration. The substrate width included the widths of the two electrodes. The paper parameters were as follows: density =1.5 g/cm^3, Young's modulus = 25 GPa, and Poisson's ratio = 0.3. The PVDF fiber parameters were as follows: fiber diameter = 5 μm, fiber length = 25 mm, piezoelectric constants of d_{31} = 20 $pC{\cdot}N^{-1}$, d_{32} = 3 $pC{\cdot}N^{-1}$, d_{33} = −33 $pC{\cdot}N^{-1}$, Young's modulus = 2.5 GPa, Poisson's ratio = 0.348, and relative dielectric constant = 8. The Al foil electrode parameters were as follows: width = 3 mm, length = 25 mm, thickness = 60 μm, density = 27 g/cm^3, Young's modulus = 70 GPa, and Poisson's ratio = 0.35. The MATLAB software was used for the numerical analyses.

3. RESULTS AND DISCUSSION

A schematic of the electrospinning setup is shown in Figure 1(a). The PVDF nanofibers were electrospun directly onto a nanogenerator device consisting of two Al foil electrodes on an insulating substrate. Conductive carbon tape was used to fix the device to the substrate. The collected nanofibers initially aligned because charge neutralization straightened them[30,31] and then randomly oriented after several nanofiber layers had been stacked because the previously collected nanofibers inhibited charge neutralization and hence prevented the electrode from continuing to act as a countercharge reservoir. Thus, it is reasonable to assume that the PVDF nanofibers were randomly oriented on the substrate. The collection drum rotation affected the nanofiber orientation only negligibly because the collection drum linear rotation speed, on the order of several meters/second, was considerably slower than the nanofiber spinning speed (e.g., several kilometers/second).[32] A schematic of the PVDF-nanofiber-based energy harvester is shown in Figure 1(b). The PVDF nanofibers were electrospun between two Al foil electrodes on the substrate, which vibrated when external sound waves induced voltage output through PVDF nanofiber dipole moments. Figure 1(c) shows an SEM image of PVDF nanofibers. The average nanofiber diameter (84.6 ± 23.5 nm) was less than that in previous work.[26] The FT-IR spectra of the nanofibers are shown in Figure 1(d). Intense peaks associated with the PVDF nanofiber β phase were at ∼470, 510, and 840 cm^{-1}, while weak peaks associated with the α phase were evident at ∼530, 610, and 763 cm^{-1}.[26] The peaks at ∼763 cm^{-1} (related to CF_2 bending and skeletal bending) and 840 cm^{-1} (related to CF_2 symmetric stretching) are characteristic of the α and β phases, respectively.[33−36] The relative β-phase fraction can be determined using the characteristic peak wavenumbers and the following equation

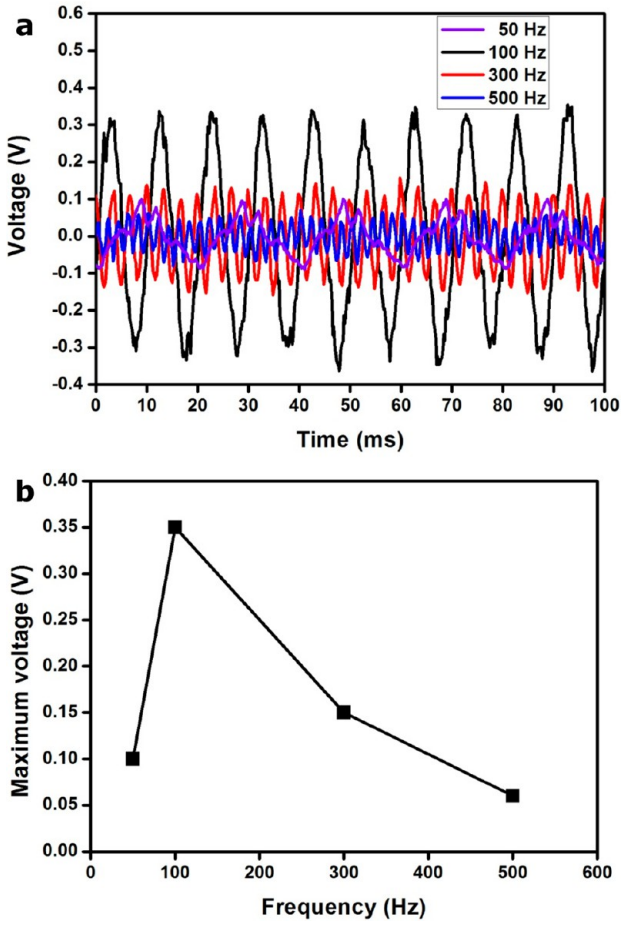

Figure 2. Frequency optimized to evaluate electrospun-PVDF-nanofiber-based energy harvester: (a) voltage-cycling-output profiles for various sound frequencies and (b) maximum voltage plotted as a function of sound frequency. The substrate was 100 μm thick PET film.

$$F(\beta) = \frac{X_\beta}{X_\alpha + X_\beta} = \frac{A_\beta}{\frac{K_\beta}{K_\alpha}A_\alpha + A_\beta} \quad (1)$$

X_α and X_β represent the degree of crystallinity of each phase; A_α and A_β represent the absorbencies of the α and β phases; and K_α and K_β are the absorption coefficients at each wavenumber and are 6.1 × 10^4 and 7.7 × 10^4 cm^2/mol, respectively.[35] The resulting relative β-phase fraction (85.2%) strongly suggests high-voltage-induced poling;[37] thus, the electrospun PVDF nanofibers were expected to be adequate for fabrication of energy harvesters.

The electrical energy converted from the sound waves was displayed as an alternating current voltage on the oscilloscope (AC input mode) because sound-wave frequencies are sinusoidal. Sound is a regular mechanical vibration that travels as a waveform through matter. Longitudinal sound waves (i.e., compression waves) transmitted through ambient air are composed of waves whose alternating pressure deviates from the equilibrium pressure, causing local regions of compression and rarefaction.[38] Flexible substrates vibrate mechanically when struck by sound waves. Transferring vibrations directly to randomly aligned PVDF fibers causes them to vibrate in turn. The sound-wave frequency was optimized to produce more significant results before evaluation of the nanogenerator

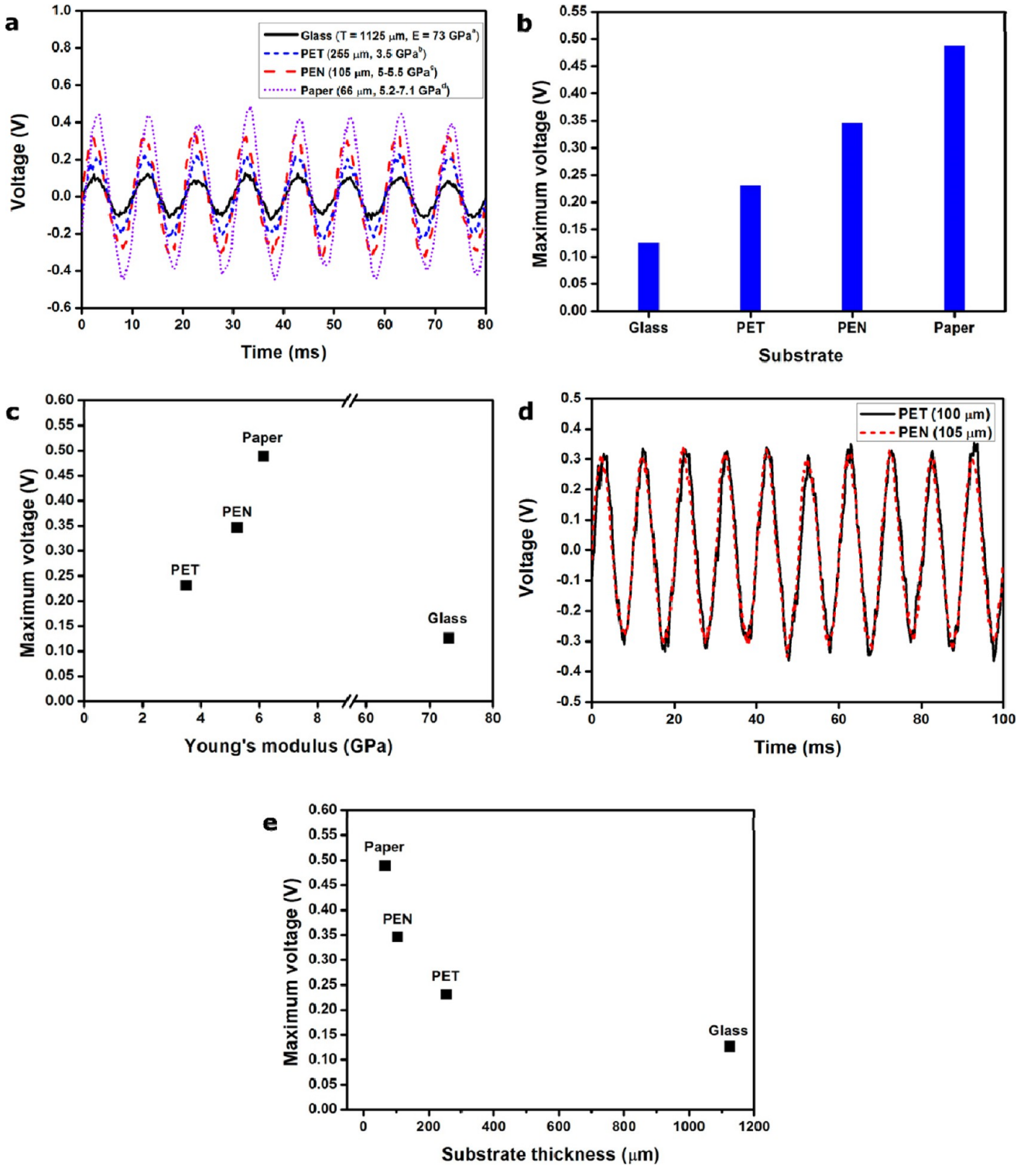

Figure 3. Sound-wave-driven voltage output according to substrate. (a) Profiles of overall voltage cycling output, (b) maximum voltage output for each substrate, (c) relationship between Young's modulus and maximum output voltage, (d) output-voltage-cycling profiles for PET (100 μm) and PEN (105 μm) films, and (e) relationship between substrate thickness and maximum output voltage. Substrate Young's moduli from [a]Paul et al.,[37] [b]Karger-Kocsis et al.,[38] [c]Sidler et al.,[39] and [d]Yokoyama et al.[40] are provided as reference values.

performance. Figure 2(a) shows the voltage cycling profiles output for various sound frequencies. The dimensions are identical to those described in the Experimental Section, and the 100 μm thick PET-film substrate was used. The sound power was 100 dB at 1 V input. The lowest frequency (50 Hz) resulted in a repeatedly stable output voltage profile, but the waveform was not sinusoidal in shape due to its small amplitude. Moreover, the amplitude of the output voltage is less than 100 mV (Figure 2(b)). At higher frequencies (300 and 500 Hz) the maximum voltages fluctuated, and the amplitudes were less than 200 mV. The fluctuation of output voltage profiles at these higher frequencies may be attributed to

dx.doi.org/10.1021/am405684m | ACS Appl. Mater. Interfaces 2014, 6, 3520−3527

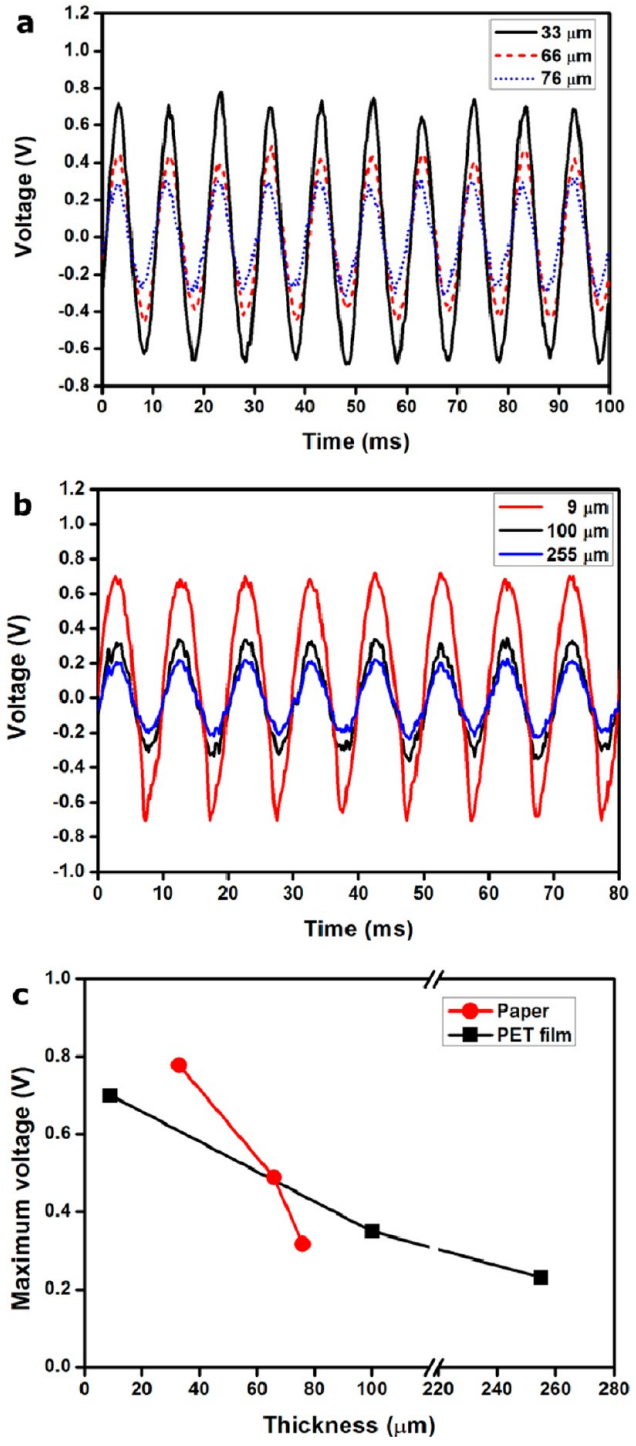

Figure 4. Relationship between substrate thickness and output voltage from PVDF nanofibers randomly aligned on paper versus PET film. Overall output voltages for (a) the paper substrate and (b) the PET substrate, as cycling continued. (c) Maximum output voltage according to substrate thickness.

a mismatch between the applied mechanical stress and the relaxation behavior of the PVDF nanofibers. Meanwhile, 100 Hz provided a highly stable oscillation and high amplitude (~350 mV). Therefore, we retained 100 Hz as the input sound-wave frequency.

The energy harvesters were fabricated simply by directly collecting PVDF nanofibers from the aluminum electrodes placed on the slide glass, PET film, PEN film, and paper substrates. During the electrospinning process, the poling axes of the PVDF nanofibers are formed along each nanofiber axis by the combined action of mechanical stretching and electrical poling. Meanwhile, the mechanical vibration of the substrate resulting from the sound wave generates an alternating tension and compression along the axis of each PVDF nanofiber. The tensile stress produces tensile strain only along the nanofiber axis, but the compressive stress results in both compressive strain along the axis and bending. Thus, it can be imagined that the 33 piezoelectric mode (longitudinal mode) becomes excited upon application of both tension and compression to the PVDF nanofibers, while the 31 piezoelectric mode (transverse mode) becomes excited only upon application of compression.[39] The bending is negligible because the length of PVDF nanofibers is predominant over their diameter. In conclusion, the 33 piezoelectric mode is excited by the sound-driven mechanical vibration, resulting in a sinusoidal output voltage. The output voltage profiles in Figure 3(a) show the effects of the various substrates on the energy harvesters. The maximum output voltages shown in Figure 3(b) increased gradually from the slide-glass- to the paper-based harvester. It can be postulated that the more a substrate is deformed the higher its output voltage. At a glance, substrate material stiffness affects deformation most significantly. Intrinsic substrate stiffness is related mainly to the Young's modulus, and extrinsic stiffness is a function of substrate thickness. As an intrinsic parameter, Young's modulus is a measure of the stiffness of a material. Note that Young's moduli for the substrate materials used in previous works are as follows: glass 73 GPa (by Paul et al.[40]), PET 3.5 GPa (by Karger-Kocsis et al.[41]), PEN 5−5.5 GPa (by Sidler et al.[42]), paper 5.2−7.1 GPa (by Yokoyama et al.[43]). A material with a lower Young's modulus will show larger deformation under the same load. By extension, a device based on a substrate with a lower Young's modulus will likely exhibit a higher sound-driven maximum voltage. The result in Figure 3(c) is, however, contradictory to this expectation. Rather, the substrate with the higher modulus showed a higher maximum voltage, with the exception of the glass substrate. This may also be caused by differences in substrate thickness. Thus, we investigated the maximum voltages of the PET film (100 μm) and PEN (105 μm) to assess the intrinsic effect more precisely (shown below). Interestingly, the cycling output voltage curves and the maximum voltages of the PET (100 μm) and PEN (105 μm) films were almost identical even though the Young's modulus of the PEN was 43−57% higher than that of the PET. (Note that the maximum voltages of the PEN (100 μm) and PEN (105 μm) were 0.3463 and 0.3498 V, respectively.) Thus, the effect of Young's modulus appears to be less important. Note that the piezoelectric performance on the styrene−butadiene−styrene (SBS) rubber substrate, which has a Young's modulus in the MPa range, was not assessed because the substrate did not vibrate in a manner synchronized with the sound wave. Thus, the substrate material requires a certain amount of elasticity for synchronization with sound waves. The nonlinear relationship between substrate thickness and output voltage (Figure 3(e)), on the other hand, is conspicuous and consistent with conventional expectations. Thinner substrates, regardless of their intrinsic stiffness, can output higher voltages, so paper (which is abundant and which showed good piezoelectric performance (Figure 3)[44,45]) is the most suitable substrate for fabrication of high-efficiency nanogenerators.

dx.doi.org/10.1021/am405684m | ACS Appl. Mater. Interfaces 2014, 6, 3520−3527

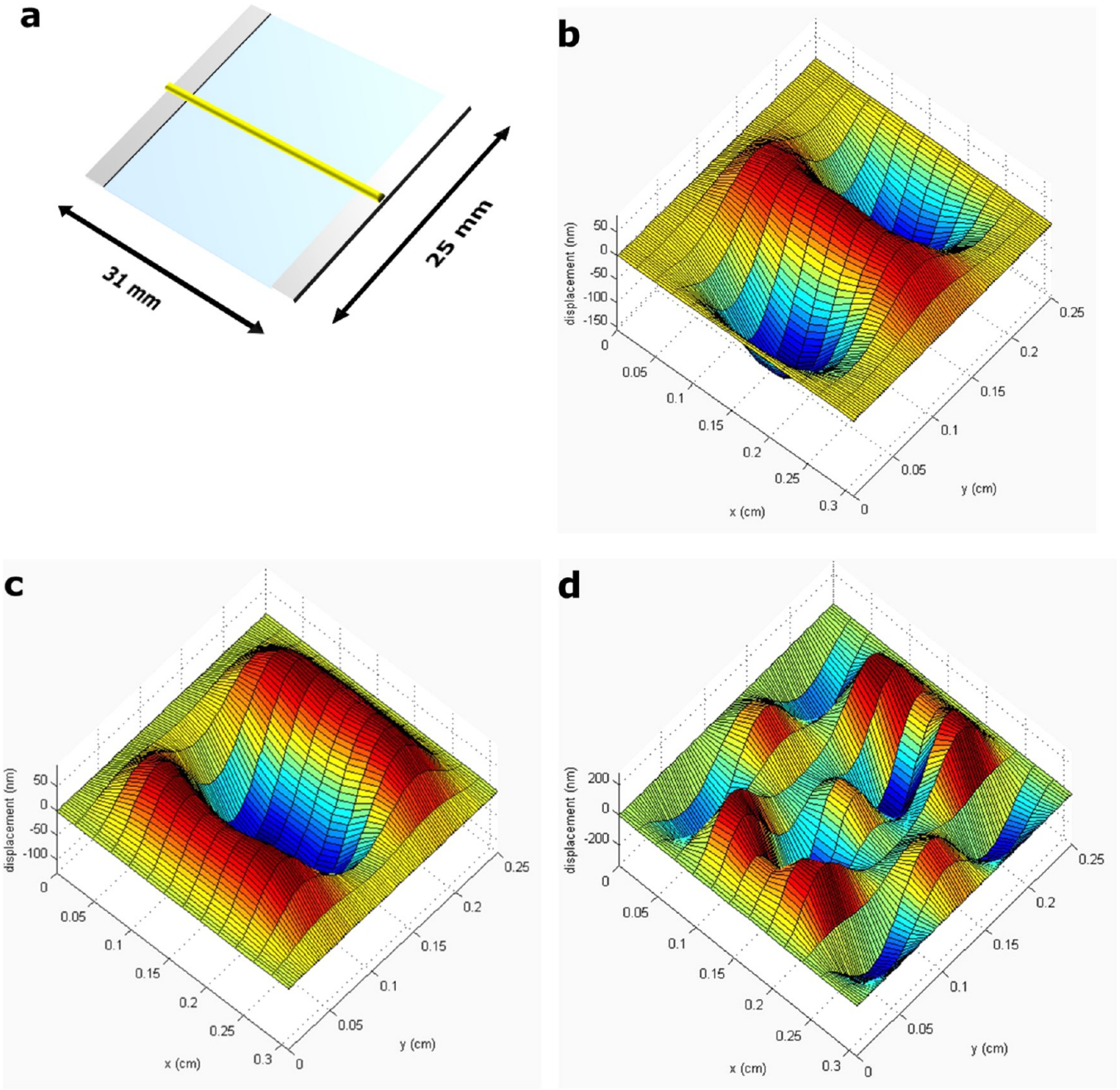

Figure 5. (a) Schematic of the paper-based nanogenerator and (b–d) the sound-wave-induced mechanical deformation profiles of (b) 76, (c) 66, and (d) 33 μm thick paper substrates.

We fabricated 76, 66, and 33 μm thick paper-based energy harvesters to evaluate the effects of paper thickness on their piezoelectricity. As shown in Figure 4(a), the output voltage amplitudes increased gradually with decreasing paper thickness. To investigate the trend and limit of the substrate thickness, we evaluated piezoelectric performance using a 9 μm thick PET film substrate and compared the results against those of substrates of 9, 100, and 255 μm thicknesses. The output waveforms shown in Figure 4(b) are sinusoidal in shape, and the maximum voltage shown in Figure 4(c) increases dramatically as the substrate thickness decreases. On the basis of the results for the 9 μm thick PET film, we expect the piezoelectric performance of PVDF nanofibers on paper thinner than 33 μm to be superior to those on a thicker substrate. As shown in Figure 4(c), the energy harvesters fabricated with the 76, 66, and 33 μm thick papers output maximum voltages of 0.3167, 0.4885, and 0.7781 V, respectively. We used a vibration model to numerically simulate the paper substrates to understand how the energy harvesters deformed in response to the sound waves.[29] The schematic in Figure 5(a) shows the paper-based device structure (i.e., the PVDF filament(s) laid across the aluminum electrodes). The detailed simulation parameters are provided in the Experimental Section. The paper-substrate harmonic deformation was relatively inhibited at a paper thickness of 76 μm. Namely, one small (<50 nm high) hill formed along the width and up toward the center, while two <150 nm deep tapered valleys formed in a downward direction. The theoretical amount of

dx.doi.org/10.1021/am405684m | ACS Appl. Mater. Interfaces 2014, 6, 3520–3527

stress applied to the PVDF filament was calculated to be 34 Pa. The 66 μm thick paper substrate harmonically deformed to a slightly greater extent: one small valley at the center and two small hills (one on each side) formed. The theoretical amount of stress applied to the filament also increased slightly to 35.3 Pa. The deformation of the 33 μm thick paper, however, was more complex and pronounced. The hills and valleys alternated widthwise and lengthwise, and the theoretical amount of stress applied to the filament improved significantly to 40.3 Pa. Consequently, paper mechanical deformation, which is a function of paper thickness, directly affects the amount of stress applied to PVDF nanofibers: thinner papers result in higher applied stresses, which produce higher output voltages.

4. CONCLUSION

PVDF-based piezoelectric energy harvesters were prepared using an electrospinning process. Electrospun PVDF nanofibers showed a high β-phase fraction due to application of a high voltage during electrospinning. The effects of various substrates and their thicknesses on the piezoelectricity of sound-driven energy generators were examined systematically using materials of various thicknesses. The thinnest (33 μm thick) paper showed the best piezoelectric performance. The numerical analyses also strongly supported the effectiveness of use of the thinnest paper substrate to fabricate energy harvesters.

AUTHOR INFORMATION

Corresponding Authors

*Phone: +82-31-280-9311. Fax: +82-31-280-6775. E-mail: jongjin00.park@samsung.com.

*E-mail: ohkim@postech.ac.kr.

Author Contributions

[+]These authors (B.-S.L. and B.P.) contributed equally to this work.

Notes

The authors declare no competing financial interest.

ACKNOWLEDGMENTS

This research was supported by the Basic Science Research Program through the National Research Foundation (NRF) of Korea funded by the Ministry of Education, Science, and Technology (2010-0022633) and the Center for Advanced Soft Electronics under the Global Frontier Research Program (2011-0031659).

REFERENCES

(1) Tabachnyk, M.; Ehrler, B.; Bayliss, S.; Friend, R. H.; Greenham, N. C. Triplet diffusion in singlet exciton fission sensitized pentacene solar cells. *Appl. Phys. Lett.* **2013**, *103* (15), 153302−153304.

(2) Lin, Z.-H.; Cheng, G.; Lin, L.; Lee, S.; Wang, Z. L. Water−Solid Surface Contact Electrification and its Use for Harvesting Liquid-Wave Energy. *Angew. Chem., Int. Ed.* **2013**, *52* (48), 12545−12549.

(3) Xie, Y.; Wang, S.; Lin, L.; Jing, Q.; Lin, Z.-H.; Niu, S.; Wu, Z.; Wang, Z. L. Rotary Triboelectric Nanogenerator Based on a Hybridized Mechanism for Harvesting Wind Energy. *ACS Nano* **2013**, *7* (8), 7119−7125.

(4) Lee, J.-H.; Lee, K. Y.; Gupta, M. K.; Kim, T. Y.; Lee, D.-Y.; Oh, J.; Ryu, C.; Yoo, W. J.; Kang, C.-Y.; Yoon, S.-J.; Yoo, J.-B.; Kim, S.-W. Highly Stretchable Piezoelectric-Pyroelectric Hybrid Nanogenerator. *Adv. Mater.* **2014**, *26* (5), 765−769.

(5) Brattstrom, B.; Bondello, M. In *Environmental Effects of Off-Road Vehicles*; Webb, R., Wilshire, H., Eds.; Springer New York: New York, NY, 1983; Chapter 9, pp 167−206.

(6) Hong, W.; Bin, X.; Xiling, L.; Jianru, H.; Shuxia, S.; Hu, L. The piezoelectric and elastic properties of berlinite and the effect of defects on the physical properties. *J. Cryst. Growth* **1986**, *79* (1−3), 227−231.

(7) Kurosawa, S.; Tawara, E.; Kamo, N.; Kobatake, Y. Oscillating frequency of piezoelectric quartz crystal in solutions. *Anal. Chim. Acta* **1990**, *230* (0), 41−49.

(8) Pinheiro, M. V. B.; Fantini, C.; Krambrock, K.; Persiano, A. I. C.; Dantas, M. S. S.; Pimenta, M. A. OH/F substitution in topaz studied by Raman spectroscopy. *Phys. Rev. B* **2002**, *65* (10), 104301.

(9) Damjanovic, D.; Demartin, M. Contribution of the irreversible displacement of domain walls to the piezoelectric effect in barium titanate and lead zirconate titanate ceramics. *J. Phys.: Condens. Matter* **1997**, *9* (23), 4943.

(10) Zhang, S.; Eitel, R. E.; Randall, C. A.; Shrout, T. R.; Alberta, E. F. Manganese-modified $BiScO_3$−$PbTiO_3$ piezoelectric ceramic for high-temperature shear mode sensor. *Appl. Phys. Lett.* **2005**, *86* (26), 262903−262904.

(11) Jung, S.-B.; Kim, S.-W. Improvement of scanning accuracy of PZT piezoelectric actuators by feed-forward model-reference control. *Precis. Eng.* **1994**, *16* (1), 49−55.

(12) Emanetoglu, N. W.; Gorla, C.; Liu, Y.; Liang, S.; Lu, Y. Epitaxial ZnO piezoelectric thin films for saw filters. *Mater. Sci. Semicond. Process.* **1999**, *2* (3), 247−252.

(13) Cha, S.; Kim, S. M.; Kim, H.; Ku, J.; Sohn, J. I.; Park, Y. J.; Song, B. G.; Jung, M. H.; Lee, E. K.; Choi, B. L.; Park, J. J.; Wang, Z. L.; Kim, J. M.; Kim, K. Porous PVDF As Effective Sonic Wave Driven Nanogenerators. *Nano Lett.* **2011**, *11* (12), 5142−5147.

(14) Fang, X.-Q.; Liu, J.-X.; Gupta, V. Fundamental formulations and recent achievements in piezoelectric nano-structures: a review. *Nanoscale* **2013**, *5* (5), 1716−1726.

(15) Sun, C.; Shi, J.; Bayerl, D. J.; Wang, X. PVDF microbelts for harvesting energy from respiration. *Energy Environ. Sci.* **2011**, *4* (11), 4508−4512.

(16) Eswaraiah, V.; Sankaranarayanan, V.; Ramaprabhu, S. Functionalized Graphene−PVDF Foam Composites for EMI Shielding. *Macromol. Mater. Eng.* **2011**, *296* (10), 894−898.

(17) Qi, Y.; Jafferis, N. T.; Lyons, K.; Lee, C. M.; Ahmad, H.; McAlpine, M. C. Piezoelectric Ribbons Printed onto Rubber for Flexible Energy Conversion. *Nano Lett.* **2010**, *10* (2), 524−528.

(18) Qi, Y.; McAlpine, M. C. Nanotechnology-enabled flexible and biocompatible energy harvesting. *Energy Environ. Sci.* **2010**, *3* (9), 1275−1285.

(19) Kawai, H. The piezoelectricity of poly (vinylidene fluoride). *Jpn. J. Appl. Phys.* **1969**, *8* (7), 975−976.

(20) Cha, S. N.; Seo, J.-S.; Kim, S. M.; Kim, H. J.; Park, Y. J.; Kim, S.-W.; Kim, J. M. Sound-Driven Piezoelectric Nanowire-Based Nanogenerators. *Adv. Mater.* **2010**, *22* (42), 4726−4730.

(21) Nalwa, H. S. In *Ferroelectric polymers: chemistry, physics, and applications*; Nalwa, H. S., Eds.; Marcel Dekker: New York, NY, 1995; Chapter 3, pp 183−232.

(22) Andrew, J. S.; Clarke, D. R. Effect of Electrospinning on the Ferroelectric Phase Content of Polyvinylidene Difluoride Fibers. *Langmuir* **2008**, *24* (3), 670−672.

(23) Yee, W. A.; Kotaki, M.; Liu, Y.; Lu, X. Morphology, polymorphism behavior and molecular orientation of electrospun poly (vinylidene fluoride) fibers. *Polymer* **2007**, *48* (2), 512−521.

(24) Zhao, Z.; Li, J.; Yuan, X.; Li, X.; Zhang, Y.; Sheng, J. Preparation and properties of electrospun poly (vinylidene fluoride) membranes. *J. Appl. Polym. Sci.* **2005**, *97* (2), 466−474.

(25) Huang, S.; Yee, W. A.; Tjiu, W. C.; Liu, Y.; Kotaki, M.; Boey, Y. C. F.; Ma, J.; Liu, T.; Lu, X. Electrospinning of polyvinylidene difluoride with carbon nanotubes: synergistic effects of extensional force and interfacial interaction on crystalline structures. *Langmuir* **2008**, *24* (23), 13621−13626.

(26) Nasir, M.; Matsumoto, H.; Danno, T.; Minagawa, M.; Irisawa, T.; Shioya, M.; Tanioka, A. Control of diameter, morphology, and structure of PVDF nanofiber fabricated by electrospray deposition. *J. Polym. Sci., Polym. Phys.* **2006**, *44* (5), 779−786.

(27) Liu, Z. H.; Pan, C. T.; Lin, L. W.; Li, H. W.; Ke, C. A.; Huang, J. C.; Wang, P. S., Eds. Mechanical properties of piezoelectric PVDF/MWCNT fibers prepared by flat/hollow cylindrical near-field electrospinning process. *Nano/Micro Engineered and Molecular Systems (NEMS), 2013 8th IEEE International Conference*; 7−10 April 2013.
(28) Chang, C.; Tran, V. H.; Wang, J.; Fuh, Y.-K.; Lin, L. Direct-write piezoelectric polymeric nanogenerator with high energy conversion efficiency. *Nano Lett.* **2010**, *10* (2), 726−731.
(29) Guminiak, M. Free vibrations analysis of thin plates by the boundary element method in non-singular approach. *Prace Nauk. Inst. Mat. Inf. Politech. Częstochow.* **2007**, *6* (1), 75−90.
(30) Hwang, K.; Yu, W.-R. Measuring tensile strength of nanofibers using conductive substrates and dynamic mechanical analyzer. *Fibers Polym.* **2009**, *10* (5), 703−708.
(31) Li, D.; Wang, Y.; Xia, Y. Electrospinning Nanofibers as Uniaxially Aligned Arrays and Layer-by-Layer Stacked Films. *Adv. Mater.* **2004**, *16* (4), 361−366.
(32) Lee, B.-S.; Kim, W.-S.; Kim, D.-H.; Kim, H.-C.; Hong, S.-H.; Yu, W.-R. Fabrication of SnO_2 nanotube microyarn and its gas sensing behavior. *Smart Mater. Struct.* **2011**, *20* (10), 105019.
(33) Zhu, H.; Mitsuishi, M.; Miyashita, T. Facile Preparation of Highly Oriented Poly (vinylidene fluoride) Langmuir−Blodgett Nanofilms Assisted by Amphiphilic Polymer Nanosheets. *Macromolecules* **2012**, *45* (22), 9076−9084.
(34) Pandey, K.; Dwivedi, M. M.; Asthana, N.; Singh, M.; Agrawal, S. L. Structural and Ion Transport Studies in (100−x) PVdF+ xNH_4SCN Gel Electrolyte. *Mater. Sci. Appl.* **2011**, *2* (0), 721−728.
(35) Gregorio, R., Jr.; Cestari, M. Effect of crystallization temperature on the crystalline phase content and morphology of poly (vinylidene fluoride). *J. Polym. Sci., Polym. Phys.* **1994**, *32* (5), 859−870.
(36) Salimi, A.; Yousefi, A. Conformational changes and phase transformation mechanisms in PVDF solution−cast films. *J. Polym. Sci., Polym. Phys.* **2004**, *42* (18), 3487−3495.
(37) Chang, C.; Fuh, Y.-K.; Lin, L., Eds. A direct-write piezoelectric PVDF nanogenerator. *Solid-State Sensors, Actuators and Microsystems Conference, 2009*. TRANSDUCERS 2009. International; 2009: IEEE.
(38) Park, B.; Lee, K.; Park, J.; Kim, J.; Kim, O. Highly Efficient Hybrid Energy Generator: Coupled Organic Photovoltaic Device and Randomly Oriented Electrospun Poly(vinylidene fluoride) Nanofiber. *J. Nanosci. Nanotechnol.* **2013**, *13* (3), 2236−2241.
(39) Tolliver, L.; Xu, T.-B.; Jiang, X. Finite element analysis of the piezoelectric stacked-HYBATS transducer. *Smart Mater. Struct.* **2013**, *22* (3), 035015.
(40) Wambua, P.; Ivens, J.; Verpoest, I. Natural fibres: can they replace glass in fibre-reinforced plastics? *Compos. Sci. Technol.* **2003**, *63* (9), 1259−1264.
(41) Karger-Kocsis, J.; Czigány, T. On the essential and non-essential work of fracture of biaxial-oriented filled PET film. *Polymer* **1996**, *37* (12), 2433−2438.
(42) Sidler, K.; Vazquez-Mena, O.; Savu, V.; Villanueva, G.; van den Boogaart, M. A. F.; Brugger, J. Resistivity measurements of gold wires fabricated by stencil lithography on flexible polymer substrates. *Microelectron. Eng.* **2008**, *85* (5−6), 1108−1111.
(43) Yokoyama, T.; Nakai, K.; Inagaki, T. Orientation Dependence of In-Plane Tensile Properties of Paper: Experiments and Theories. *J. JPS Soc. Exp. Mech.* **2009**, *9* (Special_Issue), s86−91.
(44) Kim, K.-H.; Lee, K. Y.; Seo, J.-S.; Kumar, B.; Kim, S.-W. Paper-based Piezoelectric Nanogenerators with High Thermal Stability. *Small* **2011**, *7* (18), 2577−2580.
(45) Zhong, Q.; Zhong, J.; Hu, B.; Hu, Q.; Zhou, J.; Wang, Z. L. A paper-based nanogenerator as a power source and active sensor. *Energy Environ. Sci.* **2013**, *6* (6), 1779−1784.